J Appl Electrochem (2009) 39:697–704
DOI 10.1007/s10800-008-9711-3

ORIGINAL PAPER

Effects of cathodic potential on the local electrochemical environment under a disbonded coating

Xu Chen · Cuiwei Du · Xiaogang Li ·
Yizhong Huang

Received: 15 March 2008 / Accepted: 28 October 2008 / Published online: 13 November 2008

Abstract A rectangular crevice assembly was used to investigate the effects of cathodic protection (CP) potential, bubbling CO_2 and surface condition on the crevice corrosion of X70 steel under a disbonded coating. The solution within the crevice becomes more alkaline due to the reduction of dissolved O_2. As a result, the potential of the steel reaches the protected potential range and thus the protection distance becomes longer when the applied CP potential is more negative. Potential drop (IR) mainly occurs in the vicinity of the opening. However, the introduction of CO_2 into the solution prevents the formation of an alkaline environment but gives rise to an environment with a nearly neutral pH and a uniform potential distribution in the crevice. In addition, it is found that the pre-corrosion product layer significantly decreases the polarization rate in the crevice.

Keywords X70 steel · Polarization · Cathodic protection · Crevice corrosion

X. Chen · C. Du (✉) · X. Li
School of Materials Science and Engineering, University of Science and Technology Beijing, Beijing 100083, China
e-mail: ducuiwei@yahoo.cn

X. Chen
e-mail: cx0402@yahoo.cn

X. Li
e-mail: lixiaogang99@263.net

Y. Huang
Department of Materials, University of Oxford, Oxford OX1 3PH, UK
e-mail: yizhong.huang@materials.ox.ac.uk

Abbreviations

CP	Cathodic protection
SCC	Stress corrosion cracking
SCE	Saturated calomel electrode

1 Introduction

It is common to combine both coating and cathodic protection to protect buried steel pipelines. Coating provides a barrier between the steel and environment and thus protects the pipeline steel from corrosion. However, defects such as pinholes and ruptures (so-called holidays) resulting from mechanical damage during pipeline installation may lead to the loss of adhesion of the coating to the pipeline. Water in the soil can then flow into the crevice between the pipe and the coating which reduces the bonding of the coating to the pipe. As a result, corrosion of the pipe surface occurs [1–5].

Many researchers have investigated the effects of cathodic protection (CP) on the chemical and electrochemical environment under the disbonded coating. Brousseau et al. [5] explained that the increase in pH in the crevice with time was due to the diffusion of hydroxyl ions produced by the reduction of O_2 or H_2O. Cherry et al. [6] believed that the migration of hydroxyl ions out of the crevice may be attributed to the concentration and potential gradient. The experiments of Fessler and co-workers [7] showed that the potential in the crevice was always less than the externally applied potential and therefore the crevice bottom was not fully protected. However, sufficiently negative CP may cause hydrogen evolution at the holiday. But Gan et al. [8] found, through studying the effect of CP on the steel in soils having different resistivities, that the steel could be protected with a properly controlled potential. Li et al. [9] attributed the depletion of dissolved oxygen to the cathodic current. However, Song's models [10–12] suggested that the depletion of oxygen had nothing to do with the applied cathodic current. Song suggested the increase in pH value in the crevice was caused by the reduction of water due to the remaining cathodic current. Although Perdomo et al. [13, 14] measured potential, pH and oxygen concentration within the crevice for a pipeline steel plate that was pre-corroded in aerated water, the changes in potential and pH of the pipeline steel under disbonded coating subjected to bubbling CO_2 and CP on/off have hardly been reported.

The aim of this work is to investigate the effects of CP potentials, bubbling CO_2 and the pre-corrosion product on the surface of X70 steel, on the local solution environment within the crevice. The mechanism of CP mitigating crevice corrosion is also discussed.

2 Experimental

2.1 Materials

X70 pipe steel was chosen as an experimental sample; its chemical composition is listed in Table 1. All samples were tested in a solution with a lixivium of soil. The pH of the solution was measured to be 4.6 with conductivity 0.28 mS cm^{-1}. The concentrations of the solution are given in Table 2.

2.2 Crevice cell

A simulated crevice was designed. This was a special three electrode system cell as shown schematically in Fig. 1. The cell consisted of a working electrode (i.e. polished X70 pipeline steel with dimensions of 33.5 cm × 7.5 cm × 1 cm), a saturated calomel reference electrode (SCE) with a Luggin capillary, a counter electrode, a rectangle thermoplastic shim, used to create the crevice, and a Lucite board (equivalent to a coating). The width of the crevice was controlled by the thickness of the plastic shim located between the Lucite and the steel. An opening of 3.5 cm × 1 cm was made 4 cm away from one end of the board and served as a holiday. Three ports through the Lucite block were drilled at 5 cm intervals from the holiday. These ports helped to position the microelectrodes, which were used to measure the potential of the steel plate, as well as the pH and oxygen concentration of the crevice solution. All potentials were measured against the SCE. A chamber filled with solution was assembled at the end of the Lucite board and above the holiday. Reference electrodes and counter electrodes (Pt) were placed inside the chamber.

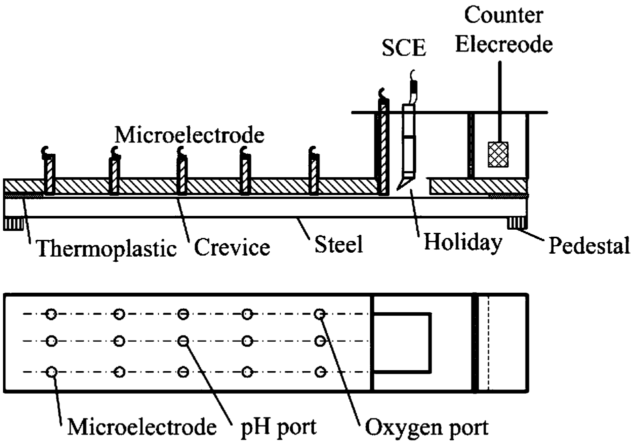

Fig. 1 The cell used to simulate a crevice under a disbonded coating

2.3 Measurement of pH and oxygen concentration

A commercially available needle-like pH electrode and a dissolved oxygen microglass electrode were used in the experiments. These were inserted into the ports in the Lucite board to carry out measurements.

2.4 Electrochemical measurement

Potentiodynamic measurements were performed using an EG&G Instrument Model 2273 through a traditional three-electrode system. The specimen was scanned from −1,200 to 400 mV at a rate of 1 mV s^{-1}. During the measurements, the solutions were purged with N_2 gas for 1 h before each potentiodynamic scan. The specimen was kept at −1,300 mV for 3 min before polarization to remove the oxide film on the surface.

Table 1 Composition of X70 steel (wt%)

C	Si	Mn	S	Cr	P	Ni	Mo	Cu	Nb	Fe
0.045	0.24	1.48	0.0001	0.031	0.017	0.16	0.23	0.21	0.033	Residue

Table 2 Physical and chemical parameters of soil (25 °C)

Cl^- (%)	SO_4^{2-} (%)	HCO_3^- (%)	NO_3^- (%)	Na^+ (%)	Mg^{2+} (%)	K^+ (%)	Ca^{2+} (%)
0.0036	0.0018	0.0011	0.0030	0.0017	0.0002	0.0006	0.0008

2.5 Bubbling CO_2 test and pre-corrosion test

First, the effect of CO_2 on the crevice corrosion of X70 steel under the coating was investigated. CO_2 was introduced into the experimental solution through purging it with 5% CO_2 and 95% N_2. The crevice corrosion was evaluated by measuring the potential distribution and pH within the crevice when the CP was applied.

During the dry season, water trapped underneath disbonded coating can vaporize and create rust (corrosion products) on the steel surfaces of pipes. In the wet season, the soil is saturated with water and seeps underneath the disbonded coating. Therefore, it is necessary to perform experiments to clarify the effect of the pre-corrosion product layer or soil lixivium on the crevice corrosion of the steel. All measurements were carried out at room temperature.

3 Results

3.1 Effect of applied cathodic potential

The effect of applied potential on the local solution environment under the disbonded coating was investigated at three potentials: −775, −1,000, and −1,200 mV. The oxygen concentration in the solution was measured to be 8.3 mg L^{-1}.

3.1.1 At −775 mV

The potential along the crevice was measured by the microelectrodes placed along the crevice when an external potential of −775 mV was applied. The potential vs time curve is shown in Fig. 2a. The potential fell immediately to approximately −775 mV at all positions including the area of the holiday and then became stable after about 12 h. The value of the pH (Fig. 2b) within the crevice was measured to be 10 at the holiday area, 5, 10 and 15 cm from the holiday. However, it was 7 at 25 cm from the holiday. The oxygen concentration within the crevice (Fig. 2c) at different positions decreased rapidly within the first 10 h and then tended to be stable.

3.1.2 At −1,000 mV

Figure 3a shows the potential-time curves at different positions when a potential of −1,000 mV was applied. The results show the potential at the holiday area increased with polarization time. This is different from the positions inside the crevice, where the potential decreased quickly with time. However, all potentials became stable after 20 h but stabilized at different values. It was also found that this potential increased along the steel plate from the mouth towards the bottom of the crevice. After 58 h polarization, the CP applied to the electrode was deliberately switched off, except for 25 cm, the potential was found to suddenly rise up to a point and keep increasing until the maximum. After that, the potential dropped back to the previous value and became constant until the applied CP was turned back

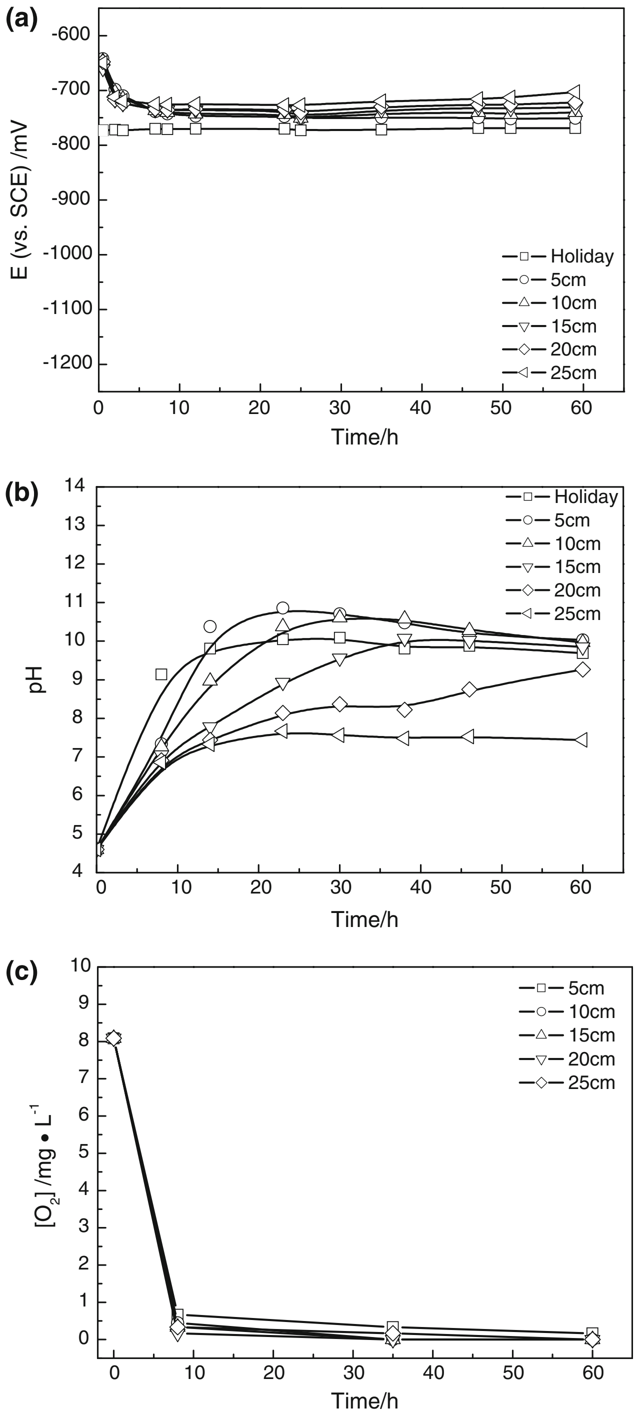

Fig. 2 Potential of the steel (**a**), pH (**b**), oxygen concentration (**c**) curves along crevice area versus time when the potential of −775 mV applied to the steel plate

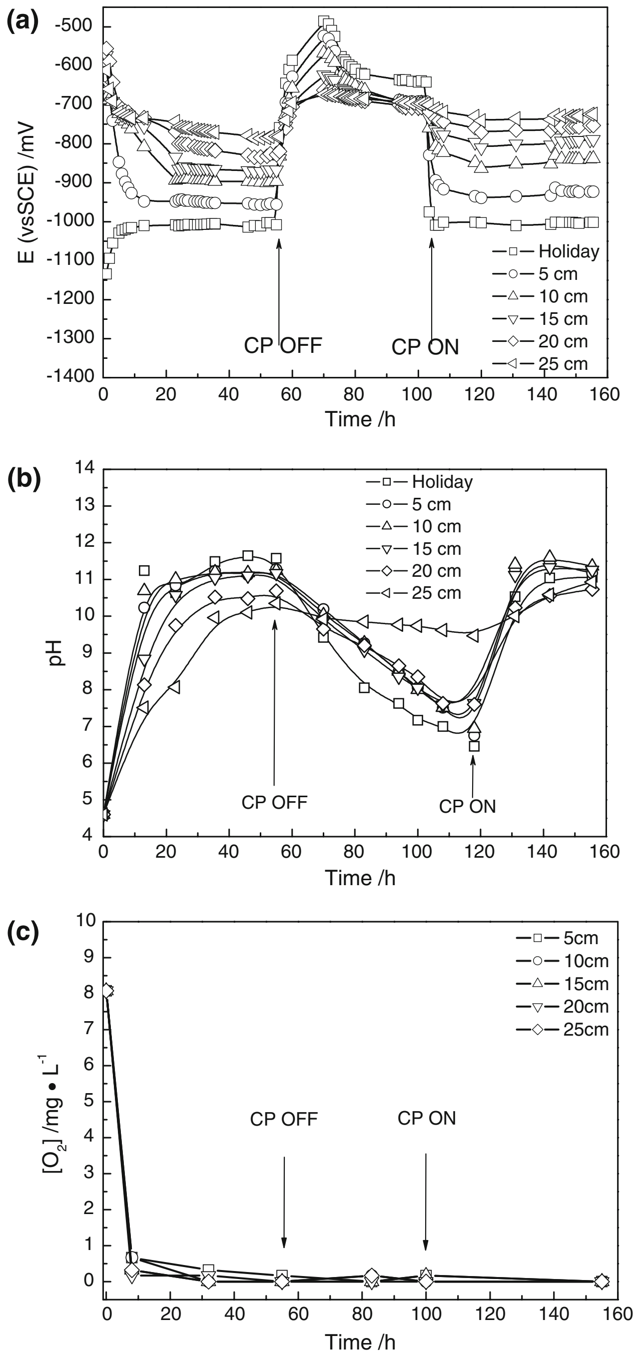

Fig. 3 Potential of the steel (**a**), pH (**b**), oxygen concentration (**c**) curves along crevice area versus time when the potential of −1,000 mV applied to the steel plate

on after 61 h. Subsequently, the potential immediately decreased and returned to the previous value before the potential was turned off. The pH at the various positions as a function of time while the potential was switched on and off is shown in Fig. 3b. It is seen that the pH increased initially and then became fairly stable but rapidly decreased when the CP was off and then rose again after the CP was turned back on. The pH was found to depend on the position. When the CP was on, at the holiday area the pH had its maximum value and decreased towards the bottom of crevice. However, it is interesting to note that when the CP was off the pH had a minimum value at the holiday area and increased towards the bottom of the crevice. Figure 3c shows that the oxygen concentration was hardly affected while the CP was turned off and on.

3.1.3 *At −1,200 mV*

At −1,200 mV many small bubbles were generated at the holiday area and the 5 and 10 cm positions. Figure 4a shows the potential-time curve. The potential at the holiday area dropped below −1,300 mV and the potential in the crevice fluctuated due to the generation of hydrogen. The pH values in the crevice (up to 11) were fairly identical and independent of position (Fig. 4b). The variation of oxygen concentration (Fig. 4c) in the crevice in this case is similar to the results obtained with an external potential of −775 and −1,000 mV.

3.2 Bubbling CO_2

Figure 5a shows that the potential measured at the holiday area always remained at around −1,000 mV. All other crevice potentials stayed between values of −700 and −800 mV. The CP was turned off after the experiment had run for 60 h. Compared to the case without CO_2, the potential at the holiday area increased positively but remained almost the same at the other positions. When the CP was turned on again after 118 h, the potential at the holiday area quickly recovered and returned to −1,000 mV, although small changes were found at the other positions in the crevice. Figure 5b shows the corresponding pH distribution. In the crevice, the pH was measured to be 7, while it was kept constant at 6 throughout the entire experiment at the holiday area. Turning the CP off had no effect on the pH.

3.3 Pre-corroded steel surface

Figure 6a shows the potential of the steel with a pre-corroded surface as a function of corrosion time. The pre-corroded steel had a much slower potential drop than the steel with a clean surface. The pH values at all positions were found to increase and stabilize between 10 and 11 (Fig. 6b), whilst the oxygen concentration decreased down to a very low value between 1 and 2 mg L^{-1} (Fig. 6c).

3.4 Polarization curves

The electrochemical polarization method was carried out to characterize the electrochemical behavior of the X70 steel at different pH in deaerated solutions. The results are

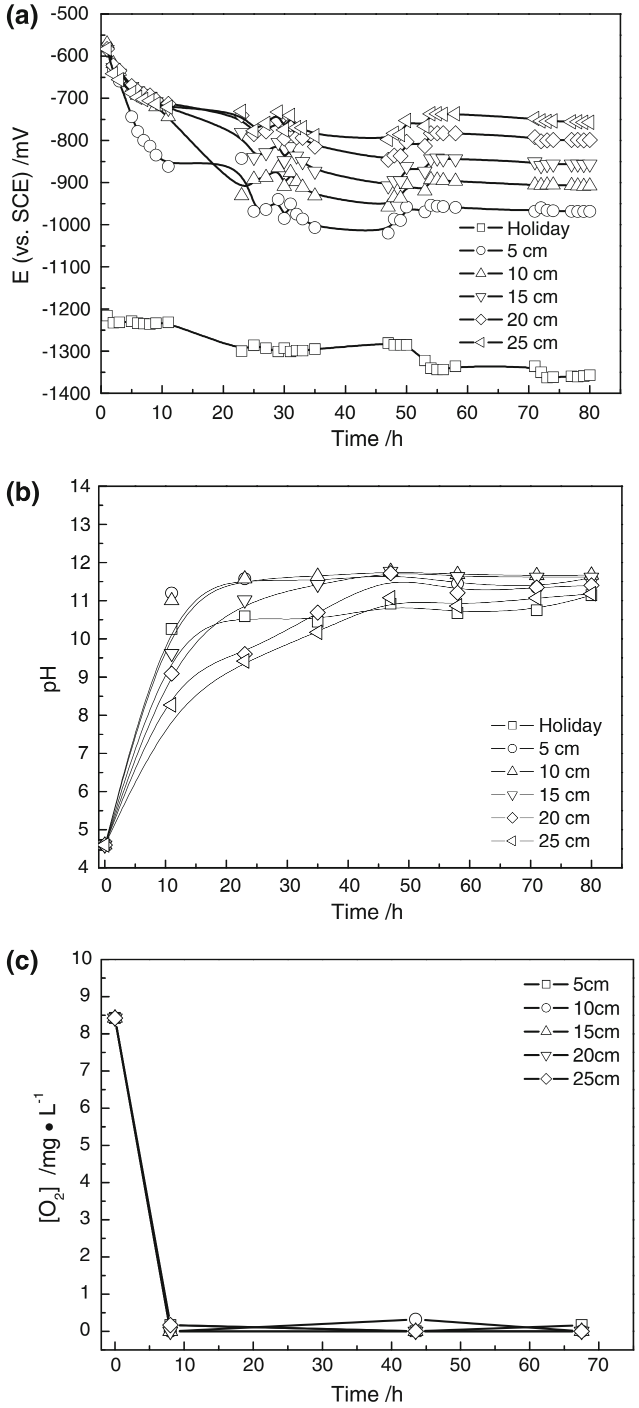

Fig. 4 Potential of the steel (**a**), pH (**b**), oxygen concentration (**c**) curves along crevice area versus time when the potential of −1,200 mV applied to the steel plate

shown in Fig. 7. In general, deaeration and alkalinity gives rise to a negative open cell potential for the steel. Therefore, when the pH is less than 9, the steel was in an active dissolution state as indicated by the anode polarization curves. The anode started to passivate and the passivation region became much wider with increase in pH.

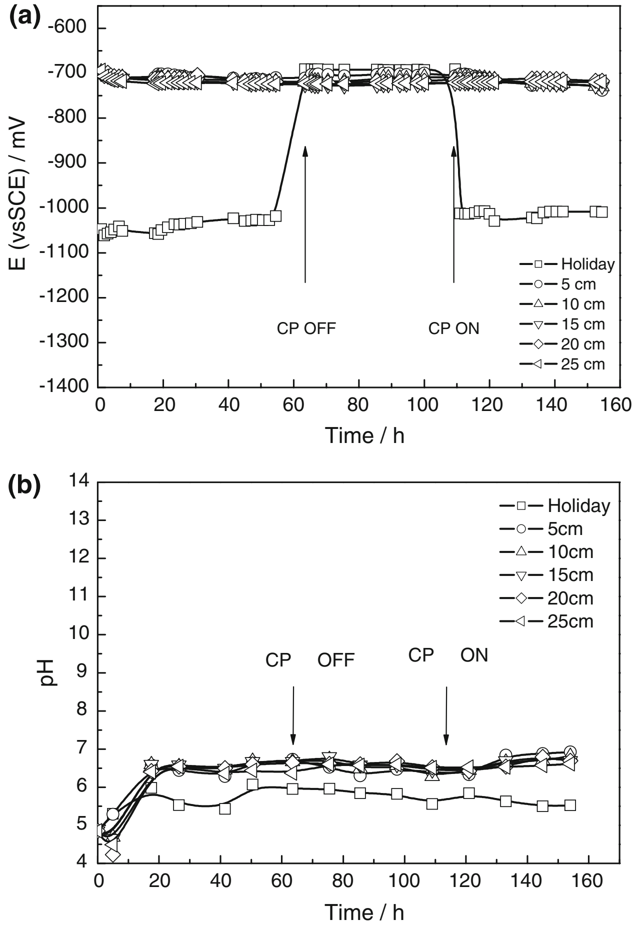

Fig. 5 Potential of the steel (**a**), pH (**b**), oxygen concentration (**c**) curves along crevice area versus time when the potential of −1,000 mV applied to the steel plate and bubbled with 5% CO_2 + 95% N_2 in the solution

4 Discussion

4.1 Potential distribution

The results show that the polarization potential in the crevice always decreases with a decrease in the applied potential. However, the conductivity of the soil lixivium is so low that the cathodic current could not reach the crevice bottom. According to the polarization measurements, both oxygen depletion and the alkaline environment are responsible for the free corrosion potential drop resulting in anode dissolution of the steel within the crevice. When a potential of −1,200 mV is applied, a number of bubbles are generated at the holiday area due to hydrogen evolution. The bubbles prevent the cathodic current from flowing into the crevice, which causes the potential at the crevice bottom to be less than −900 mV. The IR drop in the crevice mainly occurs in the vicinity of the opening due to the special crevice structure. The potential difference ranges

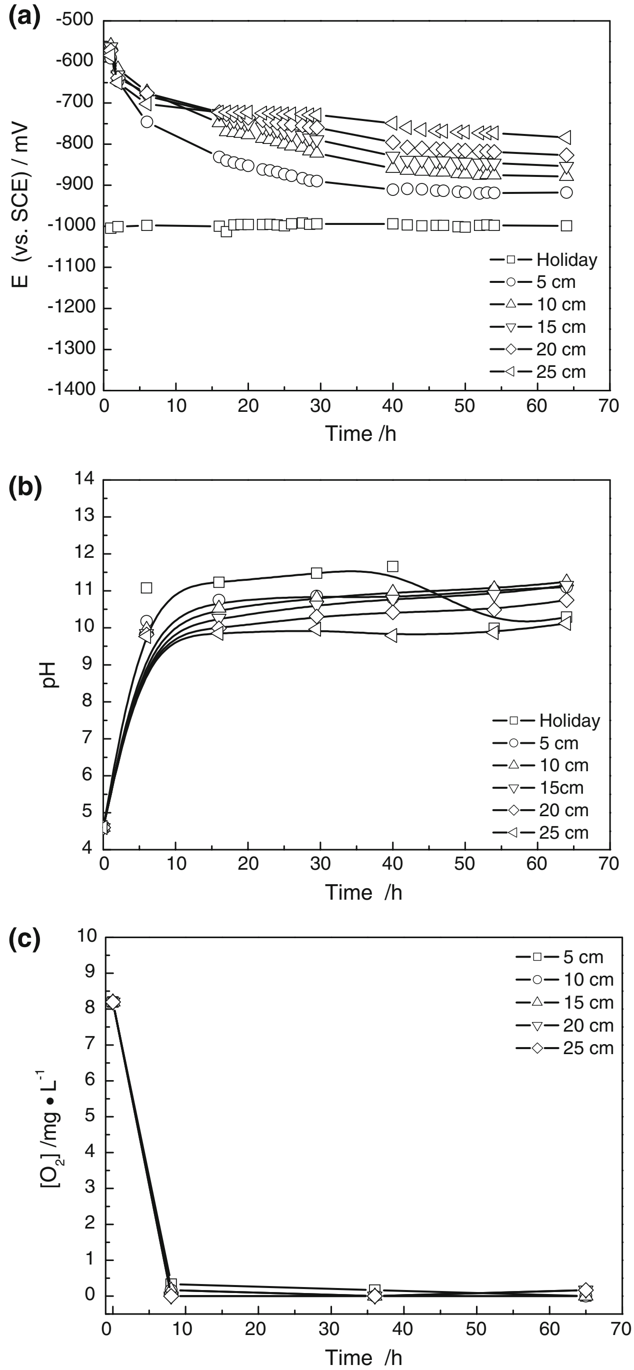

Fig. 6 Potential of the steel (**a**), pH (**b**), oxygen concentration (**c**) curves along crevice area versus time when the potential of −1,000 mV applied to the pre-corroded steel plate

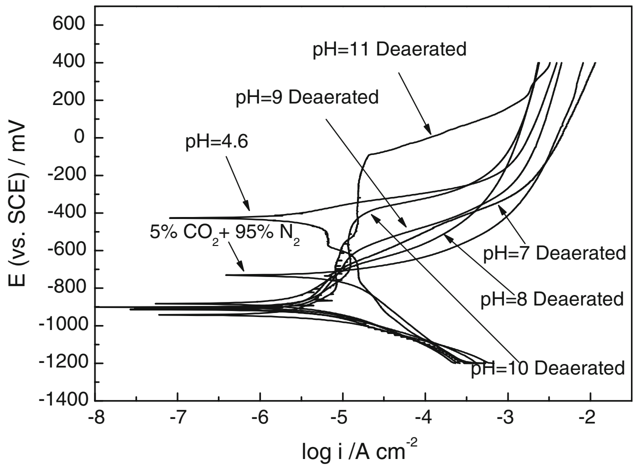

Fig. 7 Polarization curves of X70 steel with different pH

from 30 mV, with an applied potential of −775 mV, to more than 200 mV, with an applied potential of −1,200 mV.

In the case of cathodic protection, the potential in the crevice decreases with time. This implies that the cathodic current does not flow directly to all of the exposed steel [10]. This is attributed to the change in the local solution environment. The dissolved oxygen was consumed rapidly by the reaction:

$$O_2 + 2H_2O + 4e^- \rightarrow 4OH^- \quad (1)$$

Since oxygen is a neutral species and diffuses very slowly, its concentration is not influenced by the change of potential [11]. Neither was its concentration affected by variation in CP. This electrochemical process leads to the difference in the oxygen concentration in the crevice and the holiday area. The oxygen diffusion rate is much smaller than the electrochemical reaction rate. Thus, the difference in oxygen concentration together with the high resistance of the solution results in the potential gradient within the crevice. The IR drop in the crevice mainly occurs in the vicinity of the opening due to the special crevice structure.

There was no other cathodic current that could flow into the crevice when the CP was switched off. Although the potential at the holiday area immediately increases to almost 500 mV, the potential at the crevice bottom remains almost constant. This is direct evidence that the polarization within the crevice is created by the difference in the oxygen concentrations. This creates a current flow between the crevice bottom and the holiday. The polarization is reduced by the external current when the applied CP is on. Furthermore, the fact that the oxygen concentration was not affected when the CP was turned off proves that the oxygen depletion had nothing to do with the applied cathodic current.

4.2 pH changes during cathodic protection

The value of the pH in the crevice increases with decrease in applied cathodic potential. As a function of time the pH initially increases rapidly and then gradually stabilises. The pH in the crevice is related to the oxygen content due to reaction (1). The different oxygen concentrations cause the pH gradient. Li [9] thought the oxygen reduction at the crevice bottom occurs at a slower rate due to the lower polarization level. As a result, the pH at the crevice bottom was lower than that at the holiday. However, the oxygen concentration profiles showed that the dissolved oxygen was depleted rapidly. Some researchers have explained the pH rise as a result of OH^- diffusion into the crevice because of the oxygen concentration gradient. But the accumulation of OH^- in the crevice would repel the anion out of the crevice and attract cations into the crevice. Thus, the subsequent increase in pH in the crevice must be the result of water reduction through the following reaction:

$$2H_2O + 2e^- \rightarrow 2OH^- + H_2 \tag{2}$$

Song [10] simulated the chemical evolution under the disbonded coating with cathodic protection and obtained the same conclusion. Moreover, the anode dissolution process is almost completely inhibited and the hydrolyze reaction which generates H^+ on the steel could not occur under cathodic polarization. At the same time, a cathodic reduction reaction would be expected under the negative electric field in the acidic solution and it also results in the pH increase [14]:

$$O_2 + 4H^+ + 4e^- \rightarrow 2H_2O \tag{3}$$

Turning the CP off has a remarkable influence on the solution environment within the crevice. When the cathodic current is turned off, there is no extra current flow into the crevice and the steel is under free corrosion conditions. The hydrolysis reactions:

$$Fe \rightarrow Fe^{2+} + 2e^- \tag{4}$$

and

$$Fe^{2+} + 2H_2O \rightarrow Fe(OH)_2 + 2H^+ \tag{5}$$

are responsible for the decrease in pH with time inside the crevice. The steel is anodically polarized due to a differential O_2 concentration cell. The positive charges carried by ferrous ions increase with the time inside the crevice, and exceed the increase in negative charges carried by anions generated from the reduction of oxygen and water. The excessive positive charges are balanced by transport into the crevice of corrosive anions (such as Cl^-, SO_4^{2-}) from bulk and the pH decreases.

4.3 Effect of CO_2

Since carbon dioxide contained in the soil comes from decaying organic matters, it is not surprising that the solution contains the species of carbon dioxide within the vicinity of pipelines. A number of studies have been performed on CO_2 corrosion. The uniqueness of CO_2 corrosion of steel includes the presence of the additional cathodic reaction due to the reduction of H_2CO_3, and deposition of iron carbonate film on the steel surface.

When CO_2 is added to an aqueous solution, it is hydrated to form the weak acid, H_2CO_3, through the reaction [15, 16]:

$$CO_2 + H_2O \rightarrow H_2CO_3 \tag{6}$$

The H_2CO_3 is then dissociated:

$$H_2CO_3 \rightarrow H^+ + HCO_3^- \tag{7}$$

and

$$H_2CO_3 \rightarrow H^+ + CO_3^{2-} \tag{8}$$

At low pH (<4), the reduction of hydrogen ions is the dominant cathodic reaction. When the pH is between 4 and 6, a new cathodic reaction becomes dominant:

$$H_2CO_3 + e \rightarrow H^+ + HCO_3 \tag{9}$$

When the solution pH is higher than 6, the cathodic reaction is controlled by the reduction of water molecules in the deaerated solution, i.e. reaction (2).

During corrosion of steel in CO_2 systems, a layer of deposited iron carbonate is formed on the steel surface through the following reaction:

$$Fe^{2+} + CO_3^{2-} \rightarrow FeCO_3 \tag{10}$$

The deposited $FeCO_3$ film reduces the surface area available for the anodic and cathodic reactions and decreases the corrosion rate. In addition, the continuous deposition of the film effectively blocks access of cathodic current to the steel surface. Therefore, the potential in the crevice does not change with time. The pH remains constant at 7 indicating there is a force resisting any increase in pH. Apparently, the changes in the chemical and electrochemical environment inside the crevice are the result of the presence of $CO_{2,}$ which accelerates hydrogen evolution and hinders the formation of an alkaline environment. Some previous reports have suggested that the near-neutral pH stress corrosion crevice (SCC) environment under the disbonded coating is the result of CP invalidation and hydrogen is introduced by water reduction [17–19]. This work suggests that near-neutral pH environment SCC is generated even when the CP is switched on and that the hydrogen is the result of H_2CO_3 dissociation.

4.4 The effect of surface state

The level of the polarization for the pre-corroded steel surface is much lower than that of the polished steel surface because the porous corrosion products in the vicinity of the holiday prevent the cathodic current from reaching the crevice. XRD shows that the rust transformation occurred from FeO(OH) to Fe_3O_4. Stratmann et al. [20], considered that rust was formed via the intermediate product Fe^{2+} in the acidic environment. In response, the Fe^{2+} generates Fe_3O_4 through the following reactions:

$$FeO(OH) + H^+ + e^- \rightarrow Fe \cdot OH \cdot OH \qquad (11)$$

and

$$Fe \cdot OH \cdot OH + 2FeO(OH) \rightarrow Fe_3O_4 + 2H_2O \qquad (12)$$

When pre-corroded steel is drying, the alkaline environment is maintained because CP is switched off. The pre-corroded production adds the micro-anode and micro-cathode areas which promote the local cell reaction during the oxygen entering the porous corrosion products. Furthermore, pre-corroded production also decreases the width of the crevice. When the acid solution filters into the crevice again, the cathodic current flows into the crevice and the pH value increases rapidly (pH = 11) through reactions (1) and (11). The oxygen concentration profiles indicate that oxygen reduction takes place in the crevice and the oxygen reduction decreases the extent of reactions (11) and (12) [21]. In alkaline environment, the majority of the oxygen is involved in the rust reduction reactions at the holiday and thus results in a constant pH within crevice.

5 Conclusion

Cathodic protection changes the local solution environmental parameters of X70 steel in crevice under disbonded coating. These include potential, pH and oxygen concentration. The potential of the X70 steel under the disbonded coating is found to decrease but the pH of the solution increases with more negative shift of the externally applied potential. The IR drop mainly occurs in the vicinity of the opening. The crevice is insufficiently protected at an applied potential of −775 mV but hydrogen evolution occurs at the holiday when the potential is −1,200 mV. However, oxygen concentration is not affected by the variation of CP. The presence of CO_2 inhibits the formation of the alkaline environment and forms a nearly neutral SCC potential-pH environment in the crevice. The pre-corrosion product layer on the steel surface results in a uniform distribution of potential. Such a layer on the steel surface also results in a reduction in the polarization rate as well as a rapid increase in the pH, followed by stabilisation.

Acknowledgements The authors are grateful for the financial support of National R&D Infrastructure and Facility Development Program of China, whose registered number is 2005DKA10400. The correction of English language by Dr. Chris Marsh is gratefully acknowledged.

References

1. Sridhar N, Dunn DS, Seth M (2001) Corrosion 57:598
2. Chin DT, Sabde GM (1999) Corrosion 55:229
3. Yan MC, Wang JQ, Han EH (2008) Corros Sci 50:133
4. Vuillemin B, Oltra R, Cottis R (2007) Electrochim Acta 52:570
5. Brousseau R, Qian S (1994) Corrosion 50:907
6. Cherry BW, Gould AN (1990) Mater Perform 29:22
7. Fessler RR, Markworth AS, Parkins RN (1983) Corrosion 39:20
8. Gan F, Sun ZW, Sabde G, Chin DT (1994) Corrosion 50:804
9. Li ZF, Gan FX, Mao XH (2002) Corros Sci 44:689
10. Song FM, Sridhar N (2008) Corros Sci 50:70
11. Song FM, Kirk DW, Graydon JW, Cormack DE (2002) Corrosion 58:1015
12. Song FM, Jones DA, Kirk DW (2005) Corrosion 61:145
13. Perdomo JJ, Song I (2000) Corros Sci 42:1389
14. Szabó S, Bakos I (2006) Corros Rev 24:39
15. Cheng YF (2005) Bull Electrochem 21:503
16. Charles EA, Parkins RN (1995) Corrosion 51:518
17. Niu L, Cheng YF (2007) Appl Surf Sci 253:8626
18. Cheng YF (2007) Electrochim Acta 52:2661
19. Niu L, Cheng YF (2007) Electrochem Commun 9:558
20. Stratmann M, Bohnenkamp K, Engell HJ (1983) Corros Sci 23:969
21. Perdomo JJ, Chabica ME, Song I (2001) Corros Sci 43:515